Table S1: Bacterial strains and plasmids

Bacterial strains	Description	Reference
Escherichia coli		
DH5α	F-φ80d*lacZ* Δ(*lacZYA-argF*) U169 *deoR*supE44Δ*lacU169* (f80*lacZDM15*) *hsdR17 recA*1 *endA1* (rk- mk+) supE44*gyrA96 thi-1 gyrA69 relA1*	[1]
BL21(DE3)p*lysS*	F- *ompT hsdS gal* (rb- mb+) DE3(Sam7 Δ*nin5 lacUV5*-T7 Gen1)	[1]
Staphylococcus aureus		
RN4220	restriction negative strain/MSSA cloning intermediate derived from 8325-4	[2]
COL	Archaic HA-MRSA strain	[3]
COL-Δ*aldA*	COL *aldA* mutant	This study
COL-Δ*aldA::pRB473-aldA*	COL *aldA* complemented strain	This study
COL-Δ*aldA::pRB473-aldAC279S*	COL *aldAC279S* complemented strain	This study
COL-Δ*sigB*	COL *sigB* mutant	[4]
Staphylococcus phage 80		[5]

Plasmids	Description	Reference
pET11b	*E. coli* expression plasmid	Novagen
pRB473	pRB373-derivative, *E. coli/ S. aureus* shuttle vector, Amp^r, Cm^r	[6]
pRB473-XylR	pRB373-derivative, *E. coli/ S. aureus* shuttle vector, containing xylose-inducible P_{Xyl} promoter Amp^r, Cm^r	[7]
pMAD	Shuttle vector for allelic exchange in *S. aureus*, Amp^r, Em^r	[8]
pET11b-*aldA*	pET11b overexpressing His_6-AldA	This study
pET11b-*aldAC279S*	pET11b overexpressing His_6-AldAC279S	This study
pRB473-*aldA*	pRB473 expressing *aldA* under P_{Xyl}	This study
pRB473-*aldAC279S*	pRB473 expressing *aldAC279S* under P_{Xyl}	This study
pMAD-Δ*aldA*	pMAD-Δ*aldA* for *aldA* mutant construction	This study

Table S2. Oligonucleotide primers

Primer name	Sequence (5’ to 3’)
aldA-for-NdeI	GGAATTCCATATGAGAGACTACACAAAGCAATAC
aldA-rev-BamHI	CGCGGATCCTTAGTGATGGTGATGGTGATGTTTAAAATATCCAGCTATAGATTTCAC
aldA-pMAD-up-for	CGCAGATCTATCTCTCAAGATGTAATGACTG
aldA-pMAD-up-rev	ATCAAATTTATTTAAAATATCCAGCCTCATTATTCTTTCACTCCTCA
aldA-pMAD-do-for	TGAGGAGTGAAAGAATAATGAGGCTGGATATTTTAAATAAATTTGAT
aldA-pMAD-do-rev	CCAGTCGACAATAGTTCACTGTTCTTAAAAAAC
aldA-pRB-for-BamHI	TAGGGATCCTCATTCTTGAGGAGTGAAAGAATAATGAGAGACTACACAAAGC
aldA-pRB-rev-KpnI	CTCGGTACCTTATTTAAAATATCCAGCTATAGATTTC
aldA-C279S-rev	TGTACCAGCTGT**AGA**TACTTGACCAGTATTATT
aldA-C279S-for	AATAATACTGGTCAAGTA**TCT**ACAGCTGGTACA
aldA-for	CCGTGGAACTTCCCTACAAA
aldA-rev	CTAATACGACTCACTATAGGGAGATGGCTTTCTACCTGCTTCGT

Restriction sites are underlined and bold bases indicate point mutations

Table S3. Structural comparison of *sa*AldA (PDB 3TY7) with other aldehyde dehydrogenases.

PDB ID	Enzyme	R.m.s.d. [Å]	Cα atoms aligned	Sequence identity / similarity [%]
3I44	*Bartonella henselae* aldehyde dehydrogenase (*bh*ADH)	1.39	438	41 / 61
4I26	*Pseudomonas fluorescens* 2-aminomuconate-6-semialdehyde dehydrogenase (*pf*AMSDH)	1.39	428	35 / 53
2WME	*Pseudomonas aeruginosa* betaine aldehyde dehydrogenase (*pa*BADH)	1.54	434	38 / 57
1WND	*Escherichia coli* aldehyde dehydrogenase (*ec*ADH)	1.50	423	34 / 51
4I8P	*Zea mays* aminoaldehyde dehydrogenase (*zm*AMADH)	1.40	435	36 / 52
4A0M	*Spinacia oleracea* betaine aldehyde dehydrogenase (*so*BADH)	1.40	433	38 / 57
3IWK	*Pisum sativum* aminoaldehyde dehydrogenase (*ps*AMADH)	1.40	432	38 / 57
4NU9	*Staphylococcus aureus* betaine aldehyde dehydrogenase (*sa*BADH)	1.40	427	39 / 58
4I9B	*Solanum lycopersicum* aminoaldehyde dehydrogenase (*sl*AMADH)	1.43	434	39 / 56
1O05	*Homo sapiens* mitochondrial aldehyde dehydrogenase (*hs*ALDH2)	1.43	426	35 / 52

Figure S1

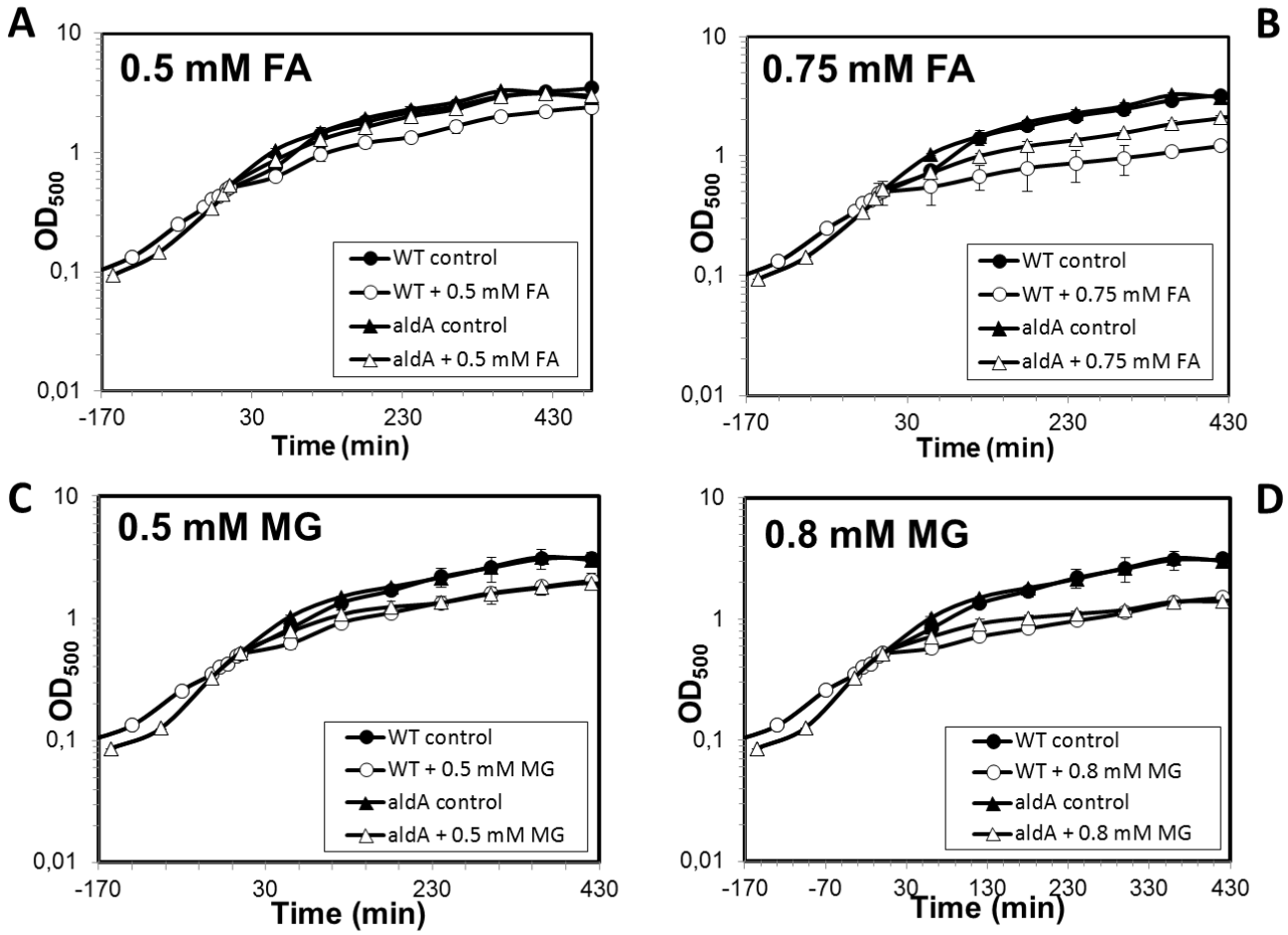

Figure S1: Growth curves of *S. aureus* COL wild type and the *aldA* deletion mutant after exposure to formaldehyde (A,B) and methylglyoxal (C,D). The *S. aureus* COL wild type and the *aldA* deletion mutant were grown in RPMI medium and exposed to sub-lethal concentrations of 0.5 mM and 0.75 mM formaldehyde **(A,B)**, 0.5 mM and 0.8 mM methylglyoxal **(C,D)** at an OD_{540} of 0.5 during the log phase. No growth phenotype of the *aldA* mutant was detected under aldehyde stress.

Figure S2

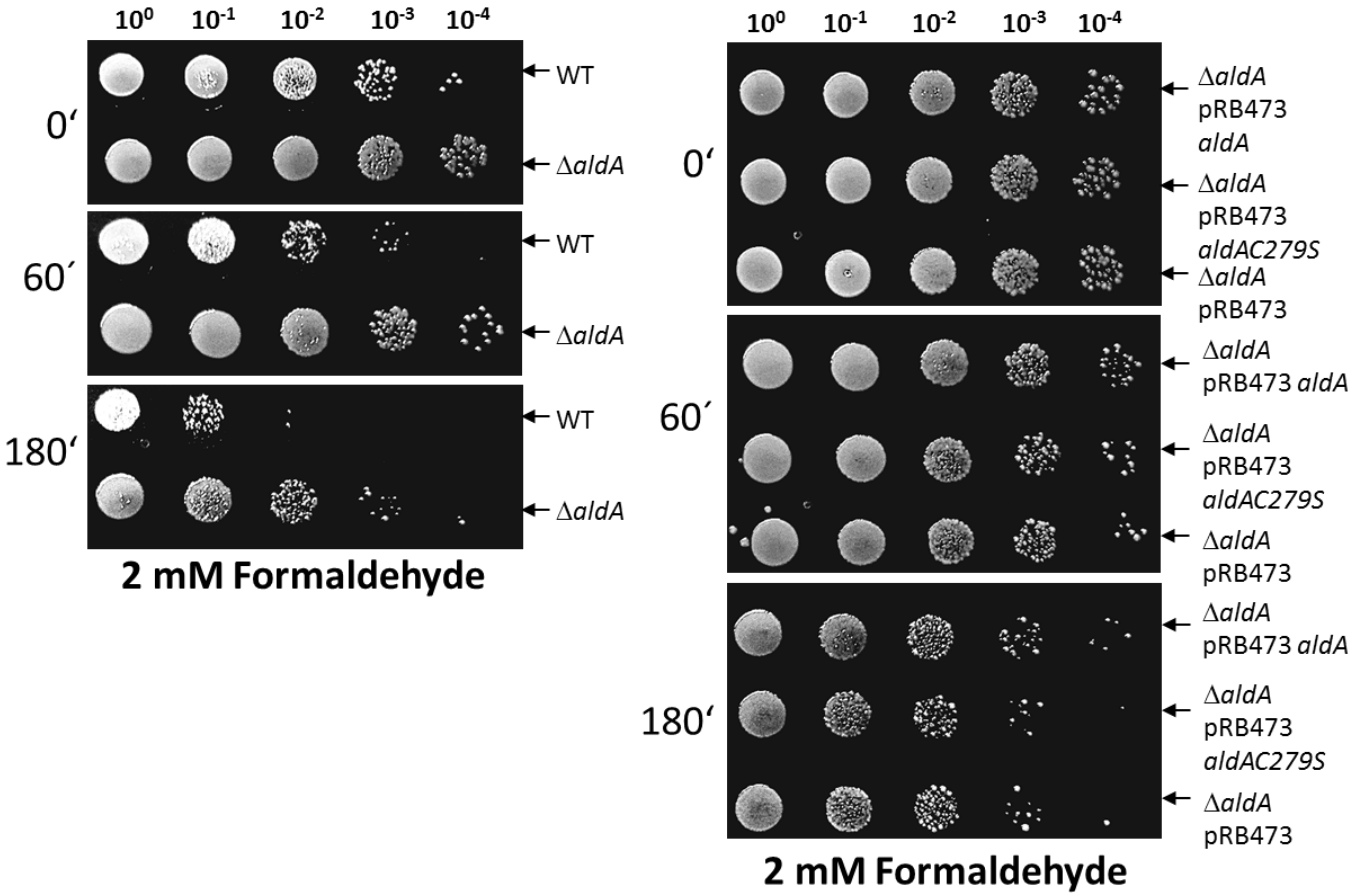

Figure S2. AldA is not required for the survival of *S. aureus* under formaldehyde stress. For the survival phenotype assays, *S. aureus* COL wild-type (WT), the Δ*aldA* deletion mutant **(A)** and the *aldA* and *aldAC279S* complemented Δ*aldA* mutants (Δ*aldA* pRB473*aldA* and Δ*aldA* pRB473*aldAC279S*) **(B)** were grown in RPMI until an OD_{500} of 0.5 and treated with 2 mM formaldehyde stress. Survival assays were performed by spotting 10 µl of serial dilutions after 1 and 3 hours of NaOCl exposure onto LB agar plates.

Figure S3

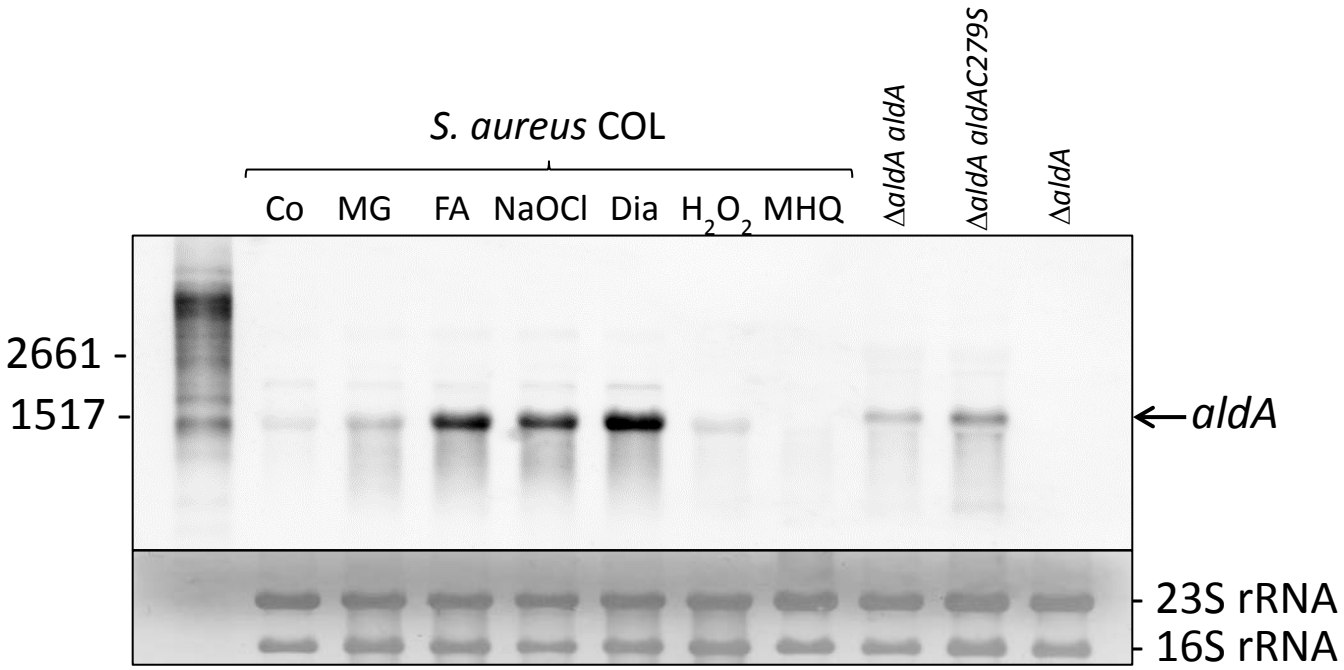

Figure S3: Transcriptional induction of *aldA* under formaldehyde, methylglyoxal, NaOCl, diamide, H_2O_2 and MHQ stress in the *S. aureus* COL wild type, Δ*aldA* mutant, *aldA* and *aldAC279S* complemented Δ*aldA* mutant strains. RNA was isolated from *S. aureus* COL wild type under control, 0.75 mM formaldehyde (FA), 0.5 mM methylglyoxal (MG), 1 mM NaOCl, 2 mM diamide, 10 mM H_2O_2 and 50 µM methylhydroquinone (MHQ) stress conditions. RNA samples were also prepared from the Δ*aldA* mutant as well as from the *aldA* or *aldAC279S* complemented strains under control conditions in the presence of 1% xylose. The RNA samples were subjected to Northern blot analysis for *aldA* (SACOL2114) transcription. The successful *aldA* and *aldAC279S* complementations are indicated. The methylene blue stain is the RNA loading control showing the abundant 16S and 23S rRNAs.

Figure S4

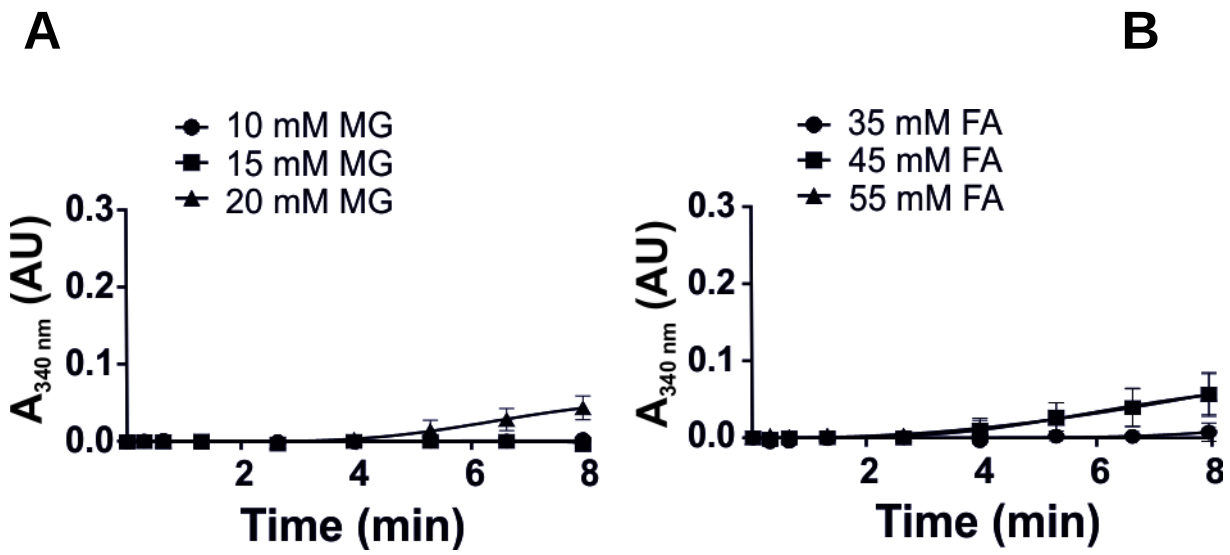

Figure S4. Cys279 is essential for AldA activity towards methylglyoxal and formaldehyde oxidation. Purified AldAC279S shows no significant activity for oxidation of methylglyoxal (MG) **(A)** and formaldehyde (FA) **(B)** and *in vitro*. Reduced AldAC279S protein (2.5 µM) was incubated with different concentrations of methylglyoxal **(A)** and formaldehyde **(B)** in reaction buffer (100 mM Tris HCl, 1.25 mM EDTA, pH 7.5). The oxidation of the aldehydes was measured in the presence of NAD^+ as coenzyme and NADH generation was monitored at 340 nm using a spectrophotometer. The results are from 3 replicate experiments. Error bars represent the SEM.

Figure S5

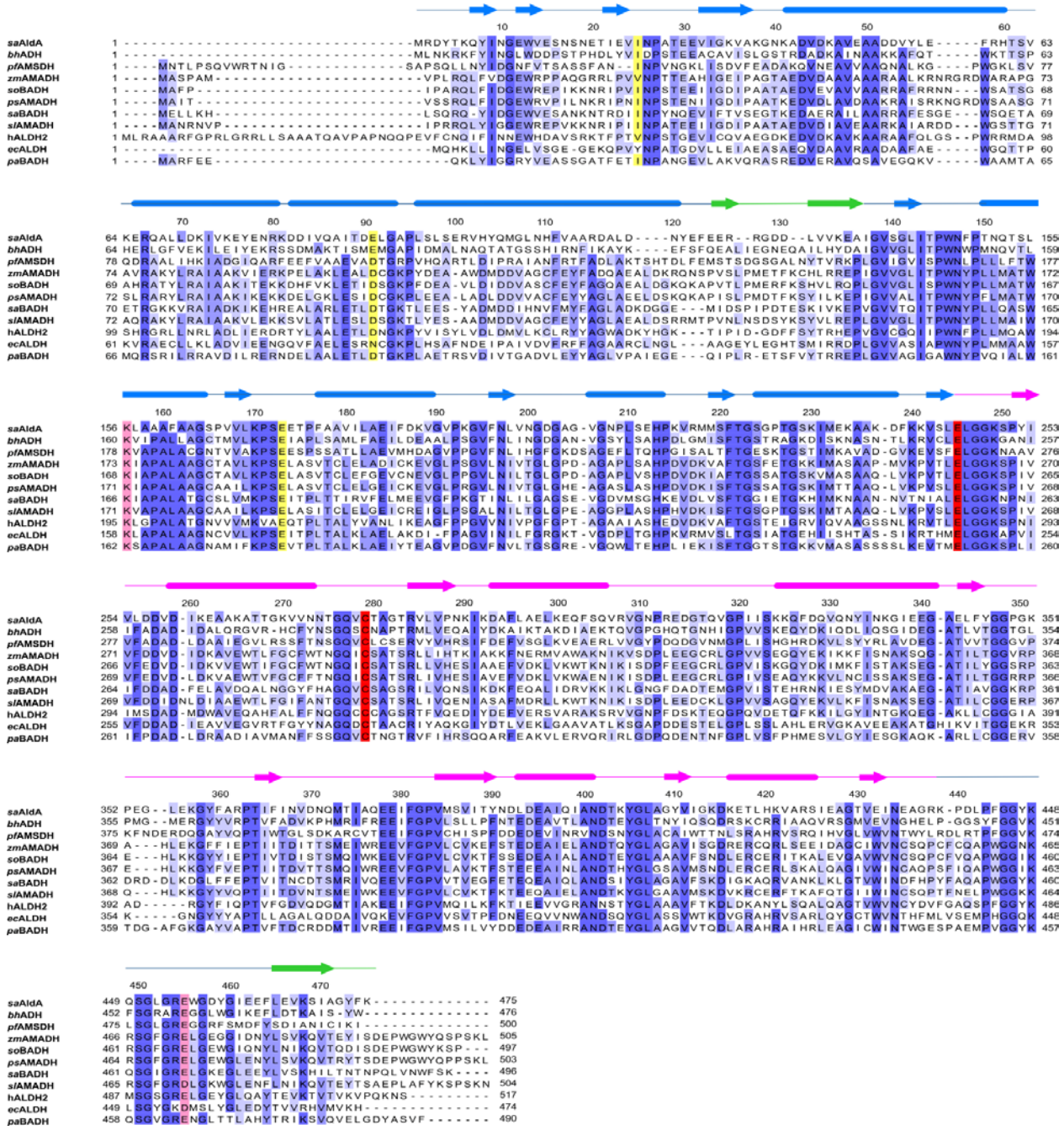

Figure S5. Sequence alignment of *sa*AldA and other ADHs (as in Table S3). Amino acid sequences were aligned using ClustalΩ [9] and presented using Jalview [10]. Intensity of the blue color gradient is based on sequence identities and similarities. The highly conserved residues are highlighted with colors (catalytic cysteine and glutamate residues – red, glutamate and lysine residues involved in catalysis – light pink; cation-binding residues – yellow). The secondary structure elements above the alignment correspond to the apo-*sa*AldA structure and are colored by domains (CoBD – blue; SID – green; CD – magenta). Numbering above the alignment is according to *sa*AldA.

Figure S6

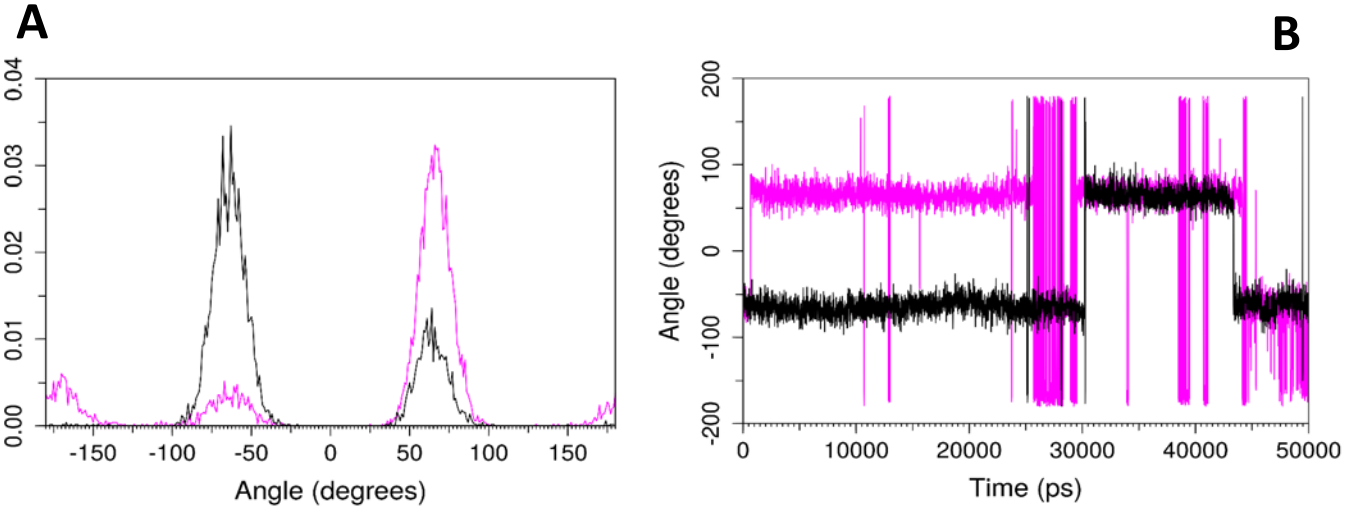

Figure S6. Plot of the dihedral distribution of N-CA-CB-SG dihedral (rotation around the CA-CB bond) of AldA Cys279 (A) and plot of the dihedral angle of AldA Cys279 in the apo- and holo-enzymes as the function of the simulation time (B). The plots show that Cys279 in the apo-enzyme **(black)** has very different dihedral propensity than in the holo-enzyme complex with NAD^+ **(magenta)**, explaining the preference of Cys279 to form the BSH complex in the apo-enzyme in the "resting" (Q2) position and in the holo-enzyme in the "attacking" (Q1) positions.

Figure S7

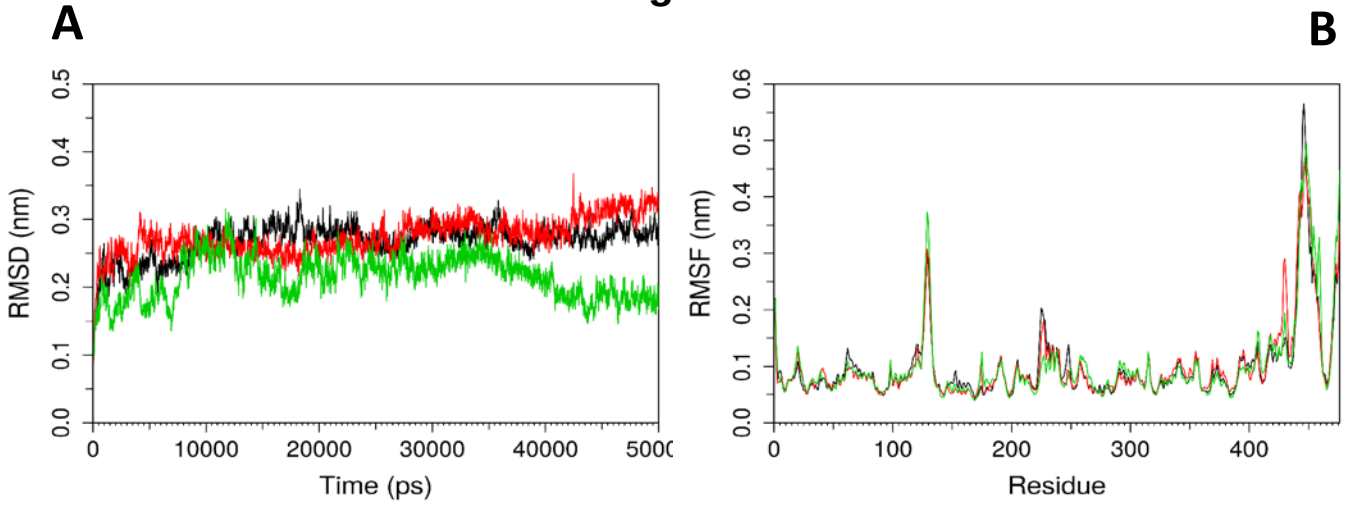

Figure S7. *S*-bacillithiolation of AldA Cys279 does not require major structural changes as revealed by MD simulations. Root-mean-square deviation (RMSD) of AldA protein backbone **(A)** and per-residue average root mean square fluctuation (RMSF) **(B)** during 50 ns of MD simulations of AldA apo-enzyme **(black)**, AldA holo-enzyme complex with BSH in "attacking" (Q1) position (red), and AldA apo-enzyme complexes with BSH in "resting" (Q2) position **(green)**. *S*-bacillithiolation resulted in little change in the backbone flexibility of AldA between the complexes of BSH with the apo-enzyme (Q2), the holo-enzyme (Q1) and the apo-enzyme without BSH.

REFERENCES

[1] Studier, F. W.; Moffatt, B. A. Use of Bacteriophage-T7 RNA-Polymerase to Direct Selective High-Level Expression of Cloned Genes. *J Mol Biol* **189:**113-130; 1986.

[2] Kreiswirth, B. N.; Lofdahl, S.; Betley, M. J.; O'Reilly, M.; Schlievert, P. M.; Bergdoll, M. S.; Novick, R. P. The toxic shock syndrome exotoxin structural gene is not detectably transmitted by a prophage. *Nature* **305:**709-712; 1983.

[3] Shafer, W. M.; Iandolo, J. J. Genetics of staphylococcal enterotoxin B in methicillin-resistant isolates of *Staphylococcus aureus*. *Infect Immun* **25:**902-911; 1979.

[4] Pane-Farre, J.; Jonas, B.; Förstner, K.; Engelmann, S.; Hecker, M. The sigmaB regulon in *Staphylococcus aureus* and its regulation. *Int J Med Microbiol* **296:**237-258; 2006.

[5] Rosenblum, E. D.; Tyrone, S. Serology, Density, and Morphology of Staphylococcal Phages. *J Bact* **88:**1737-1742; 1964.

[6] Bruckner, R.; Wagner, E.; Gotz, F. Characterization of a sucrase gene from *Staphylococcus xylosus*. *J Bact* **175:** 851-857; 1993.

[7] Pöther, D. C.; Gierok, P.; Harms, M.; Mostertz, J.; Hochgräfe, F.; Antelmann, H.; Hamilton, C. J.; Borovok, I.; Lalk, M.; Aharonowitz, Y.; Hecker, M. Distribution and infection-related functions of bacillithiol in *Staphylococcus aureus*. *Int J Med Microbiol* **303:**114-123; 2013.

[8] Arnaud, M.; Chastanet, A.; Debarbouille, M. New vector for efficient allelic replacement in naturally nontransformable, low-GC-content, gram-positive bacteria. *Appl Environ Microbiol* **70:**6887-6891; 2004.

[9] Sievers, F.; Wilm, A.; Dineen, D.; Gibson, T. J.; Karplus, K.; Li, W.; Lopez, R.; McWilliam, H.; Remmert, M.; Soding, J.; Thompson, J. D.; Higgins, D. G. Fast, scalable generation of high-quality protein multiple sequence alignments using Clustal Omega. *Mol Sys Biol* **7:**539; 2011.

[10] Waterhouse, A. M.; Procter, J. B.; Martin, D. M.; Clamp, M.; Barton, G. J. Jalview Version 2--a multiple sequence alignment editor and analysis workbench. *Bioinformatics* **25:**1189-1191; 2009.